HEAT LOAD ISSUES OF SUPERCONDUCTING UNDULATOR OPERATED AT TPS STORAGE RING*

J. C. Jan#, C. S. Hwang and P. H. Lin
NSRRC, 101 Hsin-Ann Road, Hsinchu Science Park, Hsinchu 30076, Taiwan

Abstract

For a superconducting undulator with periodic length 1.5 cm and magnet gap 5.6 mm, a magnetic flux density 1.4 T has been achieved, but heat loads from the image current of electrons in the storage ring and synchrotron radiation from the bending magnet are critical issues. The calculated power from the image current is about 3.5 W/m (RRR =60) and from the synchrotron radiation of the bending magnet is about 1.1 W (edge-field considered). This superconducting undulator will be operated at the 3-GeV TPS storage ring for which the operating current is 400 mA and the magnetic field of the dipole magnet is 1.19 T. The superconducting RF cavity will be installed in the TPS such that the bunch length is only 2.8 mm. A superconducting Landau cavity is hence necessary to extend the bunch length so as to diminish the heat load on the beam duct. Some strategies must be devised to avoid heating from the synchrotron radiation on the vacuum chamber at 4.2 K. To solve these issues, the design of the soft-end dipole and the chicane mechanism are discussed.

Introduction

The heat-load budget of a superconducting (SC) insertion device (ID) of length 1 m is an issue for the design and operation of a cryostat. The heat load on SC arrays includes not only power dissipated from the bending magnet (BMPD) and from the image current of the electron beam (ICPD) but also heat loads of conduction from the cryostat and of thermal radiation [1]. A soft-end built in the bending magnet (BM) can decrease the BMPD on the beam duct [2]. A different position of both the ID and the absorber and a different gap also influence the heat-load budget from the BMPD. The heat load of the image current depends also on the coating material (RRR ratio) on the beam duct and the parameters of the storage ring (Taiwan Light Source, TPS). The heat load due to cryostat conduction is negligible because the SC array is immersed in liquid He. Thermal radiation from the vacuum (300 K) to the beam duct (4.2 K) is also calculated.

BMPD budget

The heat-load budget of the discussed BMPD includes the full field with a normal BM, the full field with a soft-end BM and the edge field with a normal BM. In our previous work, the heat-load budget of a full field with a normal BM is 2.2 W and with a soft-end BM is 0.37 W [2]. A designed soft-end BM is displayed in Fig. 1. For a BM with a hard-end the field strength is 1.193 T and with a soft end is 0.302 T. The field strength of the soft end is a minimum (0.302T) in the pole optimization because the hard-end field leaks to the soft end. The detailed dimensions are listed in Table 1, and the calculated field strength is shown in Fig. 2(a). The pole shim and end shim are added to the pole surface and the pole side, respectively. These additions on the pole increase the region of effective field and its uniformity, displayed in Fig. 2 (b) and (c). These calculations of Fig. 2 (b) show the field uniformity plotted along the *x*-axis at the center of the hard end and soft end. Fig. 2 (c) displays the deviation of the integrated field along the *z*-axis and plotted on the *x*-axis. These results reveal that a field of satisfactory quality is provided by a soft-end BM.

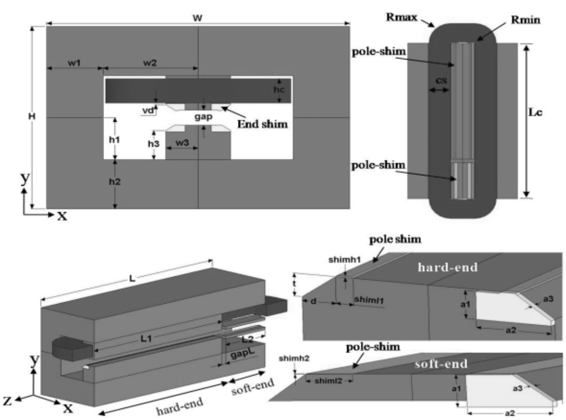

Figure 1: Sketch of hard end and soft end in the BM.

Table 1: Parameter of the soft-end

Main pole and coil		Main pole and coil	
W (mm)	806	Rmax (mm)	160
H (mm)	556.8	hc (mm)	74
L (mm)	1300	Lc (mm)	1310
L1 (mm)	970	Effective length (mm)	1110
L2 (mm)	300	cs (mm)	156
w1 (mm)	150	Rmin (mm)	4
w2 (mm)	253	J (A/mm^2)	1.95
w3 (mm)	86	By (T) @ hard-end	1.193
w4 (mm)	63	By (T) @ soft-end	0.302
h1 (mm)	128.4	**Pole-shim**	
h2 (mm)	150	shimh1 (mm)	1
h3 (mm)	89	shiml1 (mm)	12
h4 (mm)	88	shimh2 (mm)	0.26
t (mm)	16.4	shiml2 (mm)	28
d (mm)	23	**End-shim**	
vd (mm)	5	a1 (mm)	20
gap (mm)	46	a2 (mm)	51
gapL (mm)	30	a3 (mm)	5

* Work supported by the National Science Council of Taiwan for supporting this research under Contract No. NSC96-2112-M-213-006
# janjc@nsrrc.org.tw

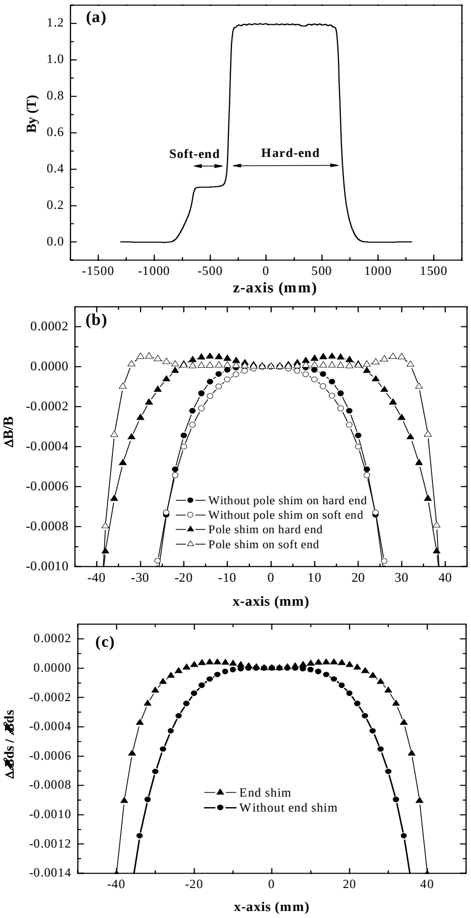

Figure 2: (a) Field strength of the hard end and the soft end, (b) A pole shim addition on the hard end and on the soft-end pole surface to increase the region of satisfactory field. (c) The end shim addition in the pole side to increase the integral field uniformity.

In the actual case, the edge field of the BM is an issue for the BMPD budget because the SR onto the beam duct is contributed mainly by the edge field of the BM. Based on the TPS design, the total angle of the electron beam trajectory bent by the BM is 0.1308 rad (7.5 deg). The distribution of the magnetic field of BM is plotted in Fig. 3. Region III is the full-field strength, 1.19 T. The curve is separated into five regions, marked I, II, III, IV and V, and fitted with a polynomial function. When the ID was placed at position B (ID after BM 6000 mm), the beam duct was irradiated with SR produced from only region V; in this region, the field strength decays rapidly. The calculated results of the edge field are listed in Table 2 with varied ID position and half gap of the absorber. Here, B_{max} is the maximum field of the SR on the beam duct. The BMPD with an absorber half gap 25 mm at A (ID after BM 4600 mm), B and C (ID after BM 8600 mm) position are 1.103, 1.057 and 0.82 W, respectively. When the absorber half gap is 20, 25 or 30 mm with an ID at position B, the BMPD is 0.684, 1.057 or 1.466 W, respectively. Generally, the Beta-function of the e-beam increased when the ID was not placed at the center of the straight section and the total impedance of the storage ring increased when the absorber gap was too small. Position B is thus selected for installation of the ID. Compared with a previous calculation for the full field, the calculated BMPD of the edge field is half that of the full field at position B with absorber half gap 25 mm.

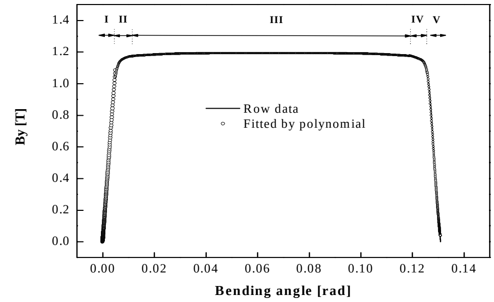

Figure 3: Contributions to the magnetic field of BM marked with I, II, III, IV and V. Regions I, II, IV and V contain the edge field. Region III is the full field.

Table 2: Estimate of BMPD with edge-field

ID position	Absorber half-gap, g1 (mm)	B_{max} (T)	Heat load on beam duct (W)
A	25	1.148	1.103
B	25	1.065	1.057
C	25	0.755	0.820
B	20	0.936	0.684
B	30	1.123	1.466

The other method to decrease the BMPD is the chicane mechanism that involves bending the e-beam with a corrector, which alters the e-beam trajectory. Two directions of the e-beam relative to the chicane include the vertical and horizontal chicane. All calculation is based on the 3-GeV TPS storage ring and the ID placed at position B, an absorber half-gap 25 mm, and assuming the beam duct to move with the e-beam chicane. Figures 4 (a) and (b) display sketches of the vertical and horizontal chicane, respectively. The original ID position is drawn with a dashed line and the moved ID position with a solid line. In the vertical-chicane, the SR on the upper-inner and lower-inner surface of the beam duct (marked by upper and lower) varies with the chicane distance, Δ. The vertical-chicane process includes (I) $\Delta < g$, (II) $\Delta > g$. When (I) $\Delta < g$, the BMPD on the upper-inner and lower-inner surface decreases and increases with Δ, respectively. When (II) $\Delta > g$, the lower-inner surface of the beam duct move over the original e-beam trajectory; there is thus no SR on the lower-inner surface of the beam duct. In the horizontal chicane, the ID moves with the e-beam chicane but the absorber is fixed on the original e-beam trajectory. Three states considered include (i) $g1 > \delta$ with $g1/a < h-\delta/(a+b+c)$, (ii) $g1 > h-\delta$ with $g1/a > h-\delta/(a+b+c)$ and (iii) $g1 < \delta$. In case (i), the SR on the inner surface is almost equivalent to that on varying with chicane distance, δ. In case (ii), the SR leaks (leak angle, θ_L) between the absorber and the beam duct, displayed in Fig. 4 (b); the BMPD is thus decreased with δ in this region. When the beam duct has larger movement in case (iii), the e-beam becomes sheltered by the absorber; assuming the absorber to move together with the beam duct is therefore necessary. Figure 5 (a) and (b) show plots of the calculated results of the vertical and horizontal-chicane, respectively. The BMPD is decreased by the vertical chicane from 9 W to 0.1 W, when the vertical-chicane distance is larger than 2.5 mm, because the beam duct move exceeds that of the original e-beam trajectory and that without SR on the lower-inner surface of the beam duct. The horizontal-chicane does not decrease the BMPD and case (ii) does not occur in our case.

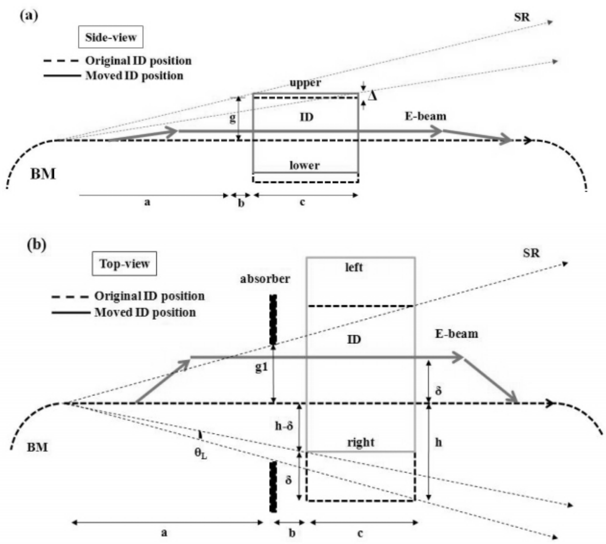

Figure 4: (a) and (b) is a diagram of vertical chicane and horizontal chicane, respectively. The dash-line and solid-line is original and after chicane of e-beam trajectory, respectively.

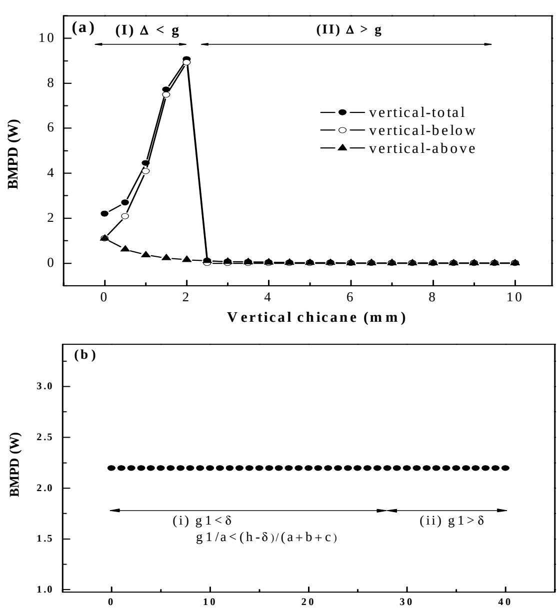

Figure 5: (a) and (b) are the BMPD calculated results after vertical chicane and horizontal chicane, respectively.

Coil heat load tolerance and thermal radiation heating

A large heat load on the cryostat consumes liquid He and causes the coil to be quenched. The load tolerance of coil heat was measured with varied magnetic field [3]. The heating tolerance is 0.79 mW/mm^2 at field strength 1.4 T. In previous work, the BMPD and ICPD are 1.1 W (edge field considered) and 3.5 W (RRR=60). The thermal radiation density was calculated according to a formula $P_R=\varepsilon\ \sigma\ (T_2^4-T_1^4)$, which ε is emissivity, σ is the Stefan-Boltzmann constant, T_1 is the temperature of the beam duct (4.2 K) and T_2 is 300 K. Thus, the power density of thermal radiation is 0.009 mW/mm^2. To compare with the measured result, the total BMPD, ICPD and thermal radiation must be changed from entire heating to local heating. In the BMPD, the maximum local heating occurs at the center with end of the beam duct. The maximum local heating of BMPD is 0.003 mW/mm^2 when the edge field considered and ID is placed at position B; an absorber half gap 25 mm was considered. Assuming the cross section of beam to be circular and of radius 2.5 mm and that the density of the ICPD is 0.223 mW/mm^2. Thus, the maximum local heating is 0.235 mW/mm^2 on the beam duct. This calculated result is less than the measurement of the coil quenching tolerance, so implying that the SC coil can safely operate in TPS.

Summary

A soft-end BM was designed that effectively decreases the BMPD. The soft-end BM was separated into a hard end and a soft end, and the field quality can be compensated with a pole shim and an end shim. The BMPD budget with a soft-end BM is 1.057 W when the absorber half gap is 25 mm and the ID is placed at position B. The discussed mechanism of a vertical chicane and a horizontal chicane shows that the vertical chicane most decreased the BMPD, but the horizontal chicane is unaffected. The heat tolerance of the coil was measured, revealing the quench heating to be 0.79 mW/mm^2 with field strength 1.4 T. As the heat for the coil quenching tolerance is greater than the calculated local heating, the SC coil can enter normal operation in TPS.

REFERENCES

[1] Erik Wallen and Greg LeBlanc, “Cryogenic system of the MAX-Wiggler”, Cryogenics 44, pp.879–893, 2004.

[2] J. C. Jan, C. S. Hwang, P. H. Lin, F. Y. Lin and C. H. Chang, "Design and Improvement of a Mini-pole Superconducting Undulator at NSRRC", MT20, Philadelphia, USA, 2007, *IEEE Trans. On Applied Superconductivity*, in press (2007).

[3] J. C. Jan, C. S. Hwang, F. Y. Lin and P. H. Lin, “The study of variety issues on the superconducting undulator” in Proceedings of the Synchrotron Radiation Instrumentation Conference, Canadian, 2008.